

UNIVERSITY OF CALIFORNIA AT BERKELEY
ASTRONOMY DEPARTMENT

REJECTION OF THE BINARY BROAD-LINE REGION INTERPRETATION OF DOUBLE-PEAKED EMISSION LINES IN THREE ACTIVE GALACTIC NUCLEI

MICHAEL ERACLEOUS^{1,2}, JULES P. HALPERN^{2,3}, ANDREA M. GILBERT,
JEFFREY A. NEWMAN, AND ALEXEI V. FILIPPENKO

Department of Astronomy, University of California, Berkeley, CA 94720

To appear in the *Astrophysical Journal*

ABSTRACT

It has been suggested that the peculiar double-peaked Balmer lines of certain broad-line radio galaxies come from individual broad-line regions associated with the black holes of a supermassive binary. We continue to search for evidence of the radial velocity variations characteristic of a double-lined spectroscopic binary that are required in such a model. After spectroscopic monitoring of three suitable candidates (Arp 102B, 3C 390.3, and 3C 332) spanning two decades, we find no such long-term systematic changes in radial velocity. A trend noticed by Gaskell (1996a) in one of the Balmer-line peaks of 3C 390.3 before 1988 did not continue after that year, invalidating his inferred orbital period and mass. Instead, we find lower limits on the plausible orbital periods that would require the assumed supermassive binaries in all three objects to have total masses in excess of $10^{10} M_{\odot}$. In the case of 3C 390.3 the total binary mass must exceed $10^{11} M_{\odot}$ to satisfy additional observational constraints on the inclination angle. We argue that such large binary black hole masses are difficult to reconcile with other observations and with theory. In addition, there are peculiar properties of the line profiles and flux ratios in these objects that are not explained by ordinary broad-line region cloud models. We therefore doubt that the double-peaked line profiles of Arp 102B, 3C 390.3, and 3C 332 arise in a pair of broad-line regions. Rather, they are much more likely to be intimately associated with a single black hole. The recent discoveries of transient but otherwise similar double-peaked emission lines in nearby AGNs bolster the view that double-peaked emission lines are commonly produced by a single compact source.

Subject headings: galaxies: active – galaxies: individual (Arp 102B, 3C 390.3, 3C 332) – lines: profiles

¹ Hubble Fellow, e-mail: mce@beast.berkeley.edu.

² Visiting Astronomer, Kitt Peak National Observatory, which is operated by AURA, Inc., under a cooperative agreement with the National Science Foundation.

³ Permanent address: Columbia Astrophysics Laboratory, Columbia University, 538 West 120th Street, New York, NY 10027.

1. INTRODUCTION

The possibility that the nuclei of radio galaxies may harbor supermassive binary black holes was suggested by Begelman, Blandford, & Rees (1980) with the purpose of explaining the observed precession of radio jets in these objects. In the original scenario, the supermassive binary would form as a result of the merger of two parent galaxies, each with its own nuclear black hole. Because radio galaxies are preferentially ellipticals, which are commonly thought to be the products of mergers, this scenario offers an appealing explanation for the proposed association of binary black holes with the nuclei of radio galaxies. The tidal perturbation of one black hole on the jet emanating from the other was the proposed origin of the jet precession. A similar idea was invoked by Wilson & Colbert (1995) who proposed that the formation of radio jets is associated with the merger of a supermassive binary. The exploration of the formation and evolution of a supermassive binary by Begelman et al. (1980) showed that for conditions typical of the nucleus of an elliptical galaxy, the supermassive binary spends most of its life (which could range between 10^8 and 10^{10} yr for black hole masses on the order of $10^8 M_\odot$) at a separation of the order of $0.01 - 0.1$ pc.

In addition to perturbing the radio jet, a second nuclear black hole may affect the dynamics of the broad-line emitting gas and hence leave an imprint on the profiles of the emission lines, as pointed out by Begelman et al. (1980) and Gaskell (1983). In particular, broad emission lines that originate in gas that is closely bound to either of the two black holes will be displaced in velocity from the rest frame of the host galaxy (as defined by either its narrow emission lines or its stellar absorption features) because of the orbital motion of the black holes about their center of mass. Gaskell (1983, 1988, 1996*a*) identified several broad-line radio galaxies as candidate hosts of supermassive binaries on the basis of either single or double displaced peaks in their broad emission-line profiles, and proposed that the binary model be applied generally to displaced emission-line peaks in active galactic nuclei (hereafter AGNs). Going one step further, Gaskell (1996*b*) and Gaskell & Snedden (1997) suggested that a large fraction of radio-loud as well as radio quiet AGNs may harbor binary black holes, objects with clearly double-peaked emission lines being the most obvious examples. The binary black hole interpretation was also discussed in favorable terms by Stockton & Farnham (1991) for the double-peaked Balmer lines of the quasar OX 169, in part because they discovered that its host galaxy appears to be an advanced merger. Additional radio-loud AGNs with double-peaked emission lines that might be treated as candidate supermassive binaries can be found in Eracleous & Halpern (1994). Those authors, however, favored an origin in a single accretion disk for the majority of the double-peaked line profiles that they found.

The most definitive observational evidence that a binary broad-line region is responsible for a double-peaked emission line would be the opposite drift of its two peaks as a result of the orbital motion of the binary black hole. Whether such a drift would be observable or not depends on the orbital period of the binary, which could range from decades to centuries. Halpern & Filippenko (1988, 1992) searched for evidence of orbital motion in two double-peaked emitters, Arp 102B and 3C 332, without success. The observed peak velocities and lower limits to their periods translate into lower limits on the masses of the binary black holes that could be responsible for binary broad-line regions in these objects. For Arp 102B and 3C 332, the derived lower limits were $4 \times 10^9 M_\odot$ and $2 \times 10^{10} M_\odot$, respectively. It was noted that if continued monitoring of the double-peaked emission lines in these two objects failed to detect orbital motion, then the mass needed under the binary broad-line region interpretation would be constrained to even larger values, ultimately rendering the binary broad-line region hypothesis untenable. In contrast to these null results, a positive result on a third broad-line radio galaxy was recently claimed by Gaskell (1996*a*), who found a systematic velocity variation in one of the two peaks of the $H\beta$ line of 3C 390.3. This was interpreted as evidence of orbital motion with a most likely period of 300 yr and a binary mass of $6.6 \times 10^9 M_\odot$.

Our continuing observational test of the binary broad-line region hypothesis for all three of these objects (Arp 102B, 3C 390.3, and 3C 332) is the subject of this paper. We use all the available data, increasing the time base on each of the three objects by at least 6 years over previously published results, thus achieving the more restrictive constraints that were anticipated by Halpern & Filippenko (1988). We discuss our (null) results in the context of other observations and theories that might be relevant to the binary black hole interpretation of double-peaked emission lines.

2. THE OBSERVATIONAL TEST

In the context of the binary black hole hypothesis, and by analogy with stellar double-lined spectroscopic binaries, we can suppose that the two peaks in double-peaked emission lines originate in ionized gas in the vicinity of each of the two black holes. We can test this supposition by searching for orbital motion of the black holes and their associated emission-line regions. Even if orbital motion is not definitely seen, a very important constraint that can be derived from the variation of the velocities of the emission-line peaks, or the lack thereof, is a lower limit on the total mass of the hypothesized binary. The two black holes are assumed to follow circular orbits around their common center of mass. Orbits are likely to be circular because dynamical friction between two parent galaxies during the merger ensures that the initial eccentricity of the resulting black hole binary is small (Polnarev & Rees 1994). An eccentricity that is small initially will not grow, and it is likely to decrease as the binary hardens (Quinlan 1996). Moreover, if the eccentricity is initially large the decay of the orbit by gravitational radiation will be accelerated, with the consequence that binaries with eccentric orbits will be much less common than ones with circular orbits (Quinlan 1996, and references therein). Any stars that happen to be in the vicinity of the supermassive binary will have a negligible effect on the potential governing the orbit of the binary. Recent estimates of the stellar mass densities in the cores of nearby, late-type galaxies ($5 \times 10^4 - 10^6 M_\odot \text{ pc}^{-3}$; Lauer et al. 1991, 1992, 1995) imply that the mass of stars within the volume occupied by the binary would not exceed $10^6 M_\odot$. This is several orders of magnitude smaller than the black hole masses that we estimate in the following sections.

We assume that the two black holes have masses and circular orbital velocities M_1, v_1 and M_2, v_2 , respectively, with a mass ratio $q = M_1/M_2 \geq 1$ by definition. It follows that the orbital velocities are related by $v_1/v_2 = 1/q$. We also define the total mass of the binary as $M = M_1 + M_2$, which is related to the orbital period P and the velocities as

$$M = \frac{1}{2\pi G} (1+q)^3 P v_1^3 \quad (1)$$

$$\text{or } M = \frac{1}{2\pi G} \left(\frac{1+q}{q}\right)^3 P v_2^3. \quad (2)$$

Unfortunately, the observer cannot measure the true orbital velocities, but instead only their projections along the line of sight, $v_1 \sin i$ and $v_2 \sin i$ (where i is the angle between the line of sight and the normal to the plane of the orbit). Assuming that the mass ratio can be measured from the line profile and that lower limits on the period and the projected orbital velocities can be obtained, equations (1) and (2) yield lower limits on the total mass of the binary as follows:

$$M > 4.7 \times 10^8 (1+q)^3 \left(\frac{P}{100 \text{ yr}}\right) \left(\frac{v_1 \sin i}{5000 \text{ km s}^{-1}}\right)^3 M_\odot \quad (3)$$

$$\text{or } M > 4.7 \times 10^8 \left(\frac{1+q}{q}\right)^3 \left(\frac{P}{100 \text{ yr}}\right) \left(\frac{v_2 \sin i}{5000 \text{ km s}^{-1}}\right)^3 M_\odot. \quad (4)$$

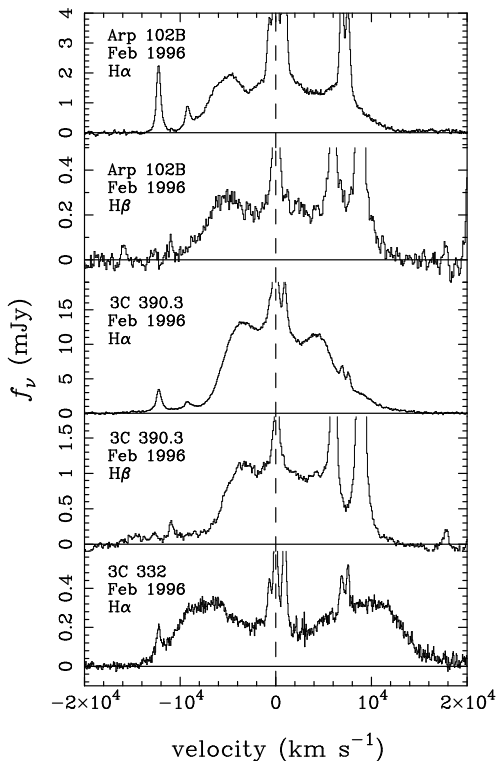


FIGURE 1— Examples of the $H\alpha$ and $H\beta$ profiles of the three target objects: Arp 102B, 3C 390.3, and 3C 332. The particular spectra shown here were obtained with the Kitt Peak National Observatory’s 2.1 m telescope in 1996 February. The $H\beta$ line of 3C 332 is not included in this figure because it is very weak and cannot provide accurate measurements of the peak velocities.

Even if the mass ratio cannot be measured, which might be the case if one of the peaks in the line profile is weak, absent, or contaminated by unrelated narrow emission-lines, a somewhat smaller (more conservative) lower limit on the total mass can still be derived because $q \geq 1$ by definition, so $(1 + q)^3 \geq 8$ and $[(1 + q)/q]^3 \geq 1$.

We apply the standard analysis of a double-line spectroscopic binary to measurements of the double-peaked $H\alpha$ lines to test the binary broad-line region hypothesis. Examples of the line profiles of the three objects on which this study focuses are presented in Figure 1. $H\alpha$ is the line of choice because it is the strongest double-peaked line, and because both of its peaks are often uncontaminated by narrow lines and hence are readily measurable. We measure the locations of both $H\alpha$ peaks wherever possible to maximize the sensitivity of the test. The $H\beta$ lines were also used, whenever available, to measure the velocity of the blue peak. Under the double-lined spectroscopic binary hypothesis, the peak with the larger velocity displacement relative to the velocity of the host galaxy is associated with the less massive black hole. The ratio of the velocities of the two peaks gives the mass ratio of the binary and is required to remain constant as the binary components revolve. The period and amplitude of the radial velocity curves can be fitted, although in practice only lower limits to both of these quantities have thus far been obtained. Such constraints are nevertheless useful because they yield lower limits to the hypothesized mass.

3. THE DATA: SPECTRA, LINE PROFILES, AND MEASUREMENTS

The observational data consist of optical spectra of the three target objects covering their $H\alpha$ and/or $H\beta$ lines. We have been accumulating spectra of these objects for about 10 years at a rate of about once per year initially and up to several times per year more recently. Our observations were carried out at Palomar Observatory, Lick Observatory, the Michigan-Dartmouth-MIT Observatory, and Kitt Peak National Observatory. A compilation of many of these spectra is shown in Eracleous (1997). Spectra taken at Lick Observatory by various observers in the 1970s and 1980s were used to

supplement our own collection. In particular, we use spectra of 3C 332 obtained by M. M. Phillips and S. A. Grandi in 1974 and 1976, and several spectra of 3C 390.3 taken by D. E. Osterbrock between 1974 and 1988. The early Lick observations of 3C 332 were originally reported by Grandi & Osterbrock (1978) and Grandi & Phillips (1979), while the early Lick spectra of 3C 390.3 were presented by Zheng et al. (1995). Measurements were also made from additional published spectra, namely the 1982 spectrum of Arp 102B presented by Stauffer, Schild, & Keel (1983), and the 1981 and 1983 spectra of 3C 390.3 presented by Oke (1987).

In Figure 1 we show examples of the $H\alpha$ and $H\beta$ line profiles of the three target objects. The $H\beta$ line of 3C 332 is not included in this figure because it is generally very weak, and thus cannot be used for accurate measurements of the peak locations. As Figure 1 shows, the $H\alpha$ lines are considerably stronger than the $H\beta$ lines and hence the $H\alpha$ profiles have a much higher signal-to-noise ratio. It is true that the telluric A- and B-bands often contaminate the $H\alpha$ line; these absorption features can routinely be corrected, however, to an accuracy that fully recovers the intrinsic $H\alpha$ line profile with the help of spectra of featureless standard stars (e.g., Wade & Horne 1988). $H\alpha$ is thus the preferred line for measuring the velocities of the twin peaks. The red peak of $H\beta$ coincides with the [O III] $\lambda\lambda 4959, 5007$ doublet and hence is not measurable. However, the $H\beta$ line is still useful since the location of its blue peak can be measured and tested for consistency with $H\alpha$. We find that the profiles of the $H\alpha$ and $H\beta$ lines are almost identical, so measurements of the blue peak of $H\beta$ can supplement those of $H\alpha$. In some of the older spectra of 3C 390.3 obtained at Lick Observatory, the telluric B-band at 6867 \AA is not corrected well, making measurements of the blue peak of $H\alpha$ unreliable. In the case of Arp 102B the red peak of $H\alpha$ cannot be measured because it coincides with the [S II] $\lambda\lambda 6717, 6731$ doublet.

We measure the velocities of the displaced peaks by fitting a symmetric, bell-shaped function to the region of the profile around the peak. By experimenting with Gaussian and parabolic fits we found that the two produce almost identical results; we adopted the Gaussian fitting method. This method locates an effective flux-weighted centroid of the profile, which does not necessarily coincide with the highest point (mode), especially if the profile is skewed. The formal uncertainty in the location of the peak is typically 100 km s^{-1} for profiles with high signal-to-noise ratio. The actual uncertainty may, however, be dominated by systematic effects of fitting a skewed profile with a symmetric function. We will return to this issue in our later discussion of the measurements. Gaskell (1996a) employed Pogson’s method for measuring the velocities of the displaced peaks (Hoffmeister, Richter, & Wenzel 1985). Gaskell’s implementation of this method (C. M. Gaskell, private communication) involves finding the midpoint between the wings (or sides) of the profile at several levels below the peak, and then locating the “center” of the profile by averaging these midpoints (in a graphical application of this technique the midpoints are averaged by fitting them with a straight line). This procedure avoids the peak of the profile because it is often skewed. Any noise in the wings of the profile can also affect the location of its peak by this method. We have compared the results of our Gaussian fitting method with the results of Gaskell’s version of Pogson’s method using several spectra of 3C 390.3 as examples. We find that the two methods give results that are in good agreement with each other. In the cases that we have tested, the mean discrepancy between the two methods is 0.6 \AA , corresponding to 30 km s^{-1} , which is smaller than the typical uncertainty with which either method can locate the velocity of a displaced peak. This justifies combining our data with those of Gaskell (1996a) in a single set. In Figures 2a and 2b we present the individual measurements of the peak velocities of Arp 102b and 3C 390.3, respectively. In the latter figure, the data used by Gaskell (1996a), which represent annual averages rather than individual measurements, are superposed for comparison. In the case of 3C 332 we only use measurements made with the Gaussian fitting method. The data are presented and discussed in the next section. The spectra and tables of measured peak velocities are presented in separate papers in which the variability of individual objects is studied in much more detail. In particular,

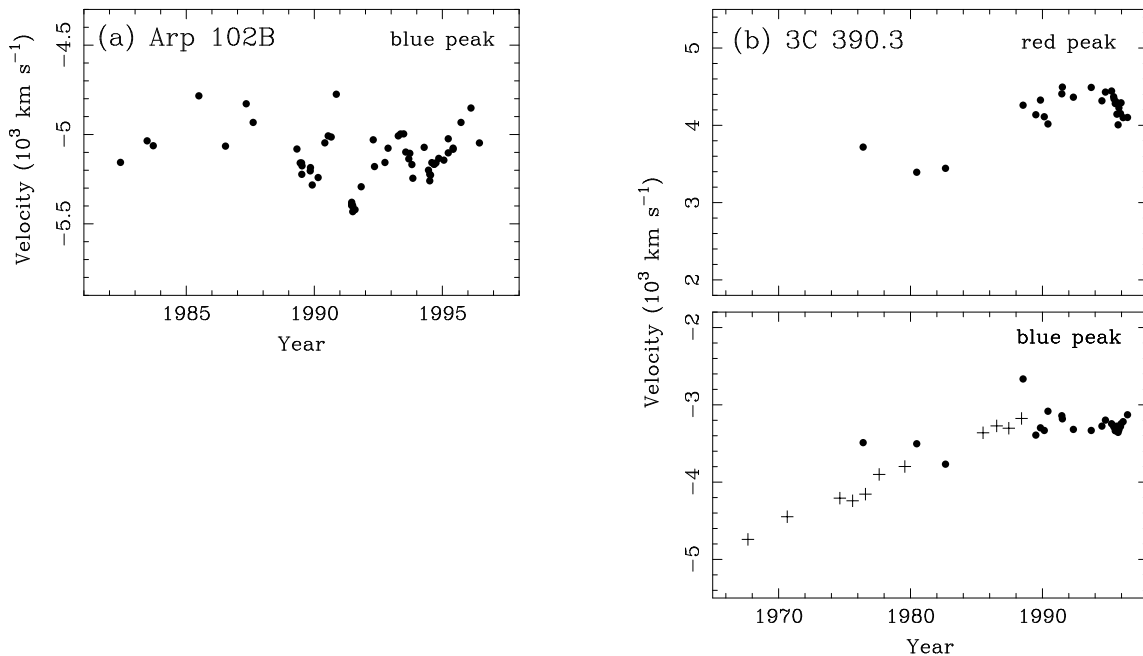


FIGURE 2— Radial velocity curves of Arp 102B and 3C 390.3 based on measurements from our spectra. Each point represents a separate measurement from an individual $H\alpha$ profile. Measurements made from the $H\beta$ profiles are omitted for clarity. Error bars are of the order of 100 km s^{-1} . The crosses in (b) show the data used by Gaskell (1996a) and are included for comparison. They represent annual averages rather than individual measurements.

the Arp 102B data are given by Newman et al. (1997), while the 3C 390.3 and 3C 332 data are given by Gilbert et al. (1997).

The radial velocities in Figure 2 show a significant scatter on short time scales (a year or less). This is a result of intrinsic changes in the detailed shape (skewness) of the profile rather than measurement uncertainties. We demonstrate this by an example below. Such profile changes trace the behavior of the line-emitting gas on time scales which are much shorter than the orbital period of the supposed supermassive binary. They could represent the reverberation of a variable ionizing continuum in the broad-line region or redistribution in phase space of line-emitting gas close to one of the two black holes on the local dynamical time scale. Under these conditions we are justified in computing annual velocity averages and using the annual dispersion as a measure of the corresponding uncertainty. This practice was also adopted by Gaskell (1996a) who presented annual average velocities of the blue $H\beta$ peak of 3C 390.3 between 1968 and 1989. By computing annual average velocities, it is thus also possible to combine our data set with that of Gaskell (1996a) and extend the temporal baseline spanned by the data on 3C 390.3. During the period 1989–1990, the line profile of 3C 390.3 displayed a very sharp blue peak as shown in Figure 3. This is a somewhat extreme but illustrative example of the type of intrinsic line profile changes that we noted above. In Figure 3 we overlay scaled versions of the 1988 and 1990 $H\alpha$ profiles of 3C 390.3 for comparison with the 1989 profile. The very shape of the 1989 profile warns against an interpretation in terms of two otherwise ordinary broad-line regions, a point to which we will

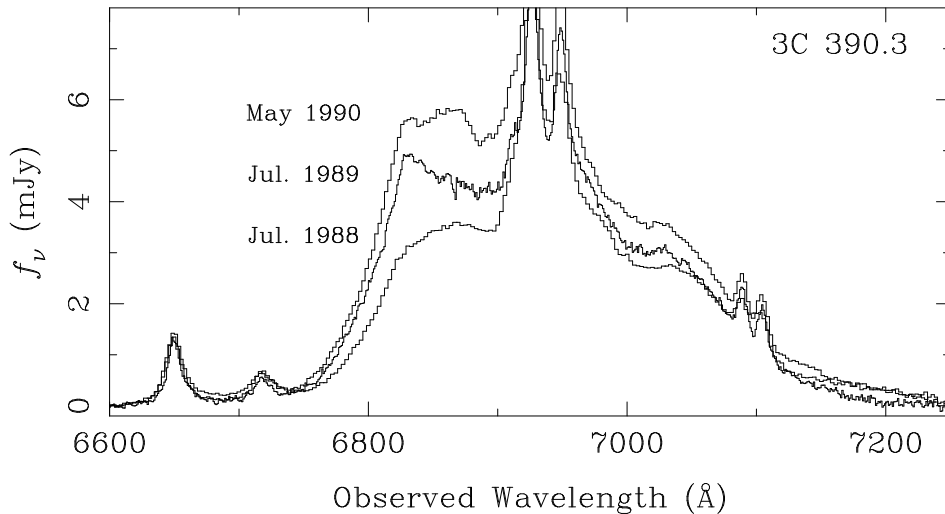


FIGURE 3 – $H\alpha$ spectrum of 3C 390.3 obtained in 1989 July, illustrating the very sharp shelf or cusp at about 6830 \AA that dominates the structure of the blueward displaced emission-line peak. For comparison we overlay the 1988 and 1990 $H\alpha$ profiles, after scaling them to an approximately equal flux in the $[O \text{ I}] \lambda 6300$ line. In addition to demonstrating the dramatic change in the shape of the profile on a short time scale, this figure also illustrates how changes in the detailed shape of the peak can affect the measurement of its “velocity.”

return in §4. However, in order to pursue the spectroscopic binary model of Gaskell (1996a) to its logical conclusion, we apply the chosen measurement techniques to this spectrum as well.

As we have noted above, the scatter in the measured velocity of a displaced peak within a year is dominated by intrinsic changes in its shape. These fluctuations have an unknown distribution, which is unlikely to be Gaussian; hence the standard error in the mean, computed according to a Gaussian theory of errors, would not reflect the true uncertainty. Thus, we have adopted the root-mean-square (r.m.s.) dispersion, computed as $\sigma = (\langle v^2 \rangle - \langle v \rangle^2)^{1/2}$, as a measure of the uncertainty in the velocity of the hypothesized black hole, rather than the error in the mean⁴. In years when only one or two measurements are available, we assigned the same error bar as in the year with the best-determined dispersion (i.e., the largest number of measurements). The error bars computed as described above were used in our further analysis, including the application of the χ^2 test. Because the adopted error bars are larger than the error in the mean (by a factor of 3 or less), the resulting values of χ^2 in the analysis presented below are correspondingly lower. As a result the lower limits on the binary masses and periods that we ultimately derive are smaller (i.e. more conservative) than what the error-in-the-mean error bars would yield. The annually-averaged radial velocity curves were compared with the predictions of the binary broad-line region model as we describe in

⁴ The error bars of Gaskell (1996a) were computed as $\sigma_n = \sigma/\sqrt{n}$ (where n is the number of measurements made within the same year); they represent the error in the mean rather than the dispersion. Because the dispersion in the annual samples of Gaskell’s data is dominated by measurement errors (C. M. Gaskell, private communication), we have retained these error bars without adjusting them to our convention.

the next section, with the goal of deriving constraints on the properties of the hypothesized binary black hole.

4. CONFRONTATION OF PREDICTIONS WITH OBSERVATIONS

To assess the applicability of the binary broad-line region model to the double-peaked Balmer lines of the target objects, we attempted to fit the radial velocity curves constructed above to the equations of the double-lined spectroscopic binary. In the convention adopted here, these equations can be written as

$$u_1(t) = (v_1 \sin i) \sin \left[\frac{2\pi}{P}(t - t_0) \right] \quad (5)$$

$$u_2(t) = - (v_2 \sin i) \sin \left[\frac{2\pi}{P}(t - t_0) \right] , \quad (6)$$

where t_0 is the time at which the observed velocity of the two peaks vanishes (inferior conjunction of the primary). In the cases where radial velocity curves for both peaks are available, these were fitted simultaneously assuming a common period and phase and allowing the two velocity amplitudes to be independent. This method, in which all of the data are used simultaneously, produces the most sensitive constraints on the model parameters. Because the period P and zero phase epoch t_0 are nonlinear parameters, the fitting algorithm scans the $P - t_0$ plane systematically. At each point the values of the velocity amplitudes ($v_1 \sin i$, $v_2 \sin i$) are computed analytically by χ^2 minimization, along with the value of χ^2 itself. The $P - t_0$ plane is explored thoroughly in order to find the asymptotic behavior of the model parameters at very long periods.

The resulting χ^2 surface is used to find the best fit through the velocity curves as well as to set limits on the model parameters (see Lampton, Margon, & Bowyer 1976). In particular, we determine the shortest period that is consistent with the data (at 99% confidence) along with the corresponding velocity amplitudes. The velocity amplitudes are linear parameters in the model adopted here; hence their optimal values and confidence limits can be computed analytically at every point in the $P - t_0$ grid. These are essential ingredients for constraining the mass of the binary according to inequalities (3) and (4). The mass ratio is also determined; it is the ratio of the best-fitting radial velocity amplitudes.

The algorithm described above was used to fit the annually-averaged radial velocity curve for each object (see §3). In Figure 4 we show these velocity curves, with the best fitting binary orbit models superposed. As this figure shows, the best-fitting orbital motion models provide very poor descriptions of the data. The reduced χ^2 values corresponding to these fits are considerably larger than unity (see Table 1), and thus the models are formally rejected with very high confidence (even with the generous error bars used). Moreover, in the case of 3C 390.3 and 3C 332, the variability does not even approximate the behavior of a spectroscopic binary. The two peaks do *not* drift in opposite directions, and as a result the instantaneous velocity ratio fluctuates considerably. If we insist on following the binary black hole hypothesis to its logical conclusion, we would have to allow for the existence of an additional source of noise superimposed on the radial velocity curve that is larger than our original error bars. We have investigated whether we can compensate for this hypothetical shortcoming of our error analysis by renormalizing the reduced χ^2 surface to unit minimum. This is equivalent to enlarging all error bars until the radial velocity model of equations (5) and (6) becomes consistent with the data. But then the 99%-confidence lower limit on the orbital period from the renormalized χ^2 surface produces a fit that bears even less resemblance to the original data, essentially because any evidence for binary motion is lost in the much larger noise

TABLE 1: LOWER LIMITS ON BINARY ORBIT PARAMETERS ^a

	Arp 102B	3C 390.3	3C 332
χ^2_{ν} (d.o.f.)	8.54 (10)	18.5 (20)	0.74 (9)
Mass Ratio	1.5 ^b	1.20	1.33
Best-Fitting Period (yr)	390	∞	144
Minimum Period (yr)	159	811	82
Minimum Total Mass (M_{\odot})	1.3×10^{10}	4.2×10^{10}	1.5×10^{10}
Minimum Orbital Separation (pc)	0.34	1.47	0.23

^a Minimum orbital periods are derived by fitting the annually averaged velocity curves, and correspond to the 99% confidence levels in the appropriate χ^2 surface. The minimum mass and minimum orbital separation are then derived from the minimum period and the fitted velocity amplitude. The most conservative (lowest) limits are listed here.

^b The mass ratio for Arp 102B cannot be measured precisely because its red peak is contaminated by the [S II] lines. We estimate $q \approx 1.5$, which we use to derive the limits quoted here.

of unknown origin. For this reason, we have little confidence in the validity of this renormalization procedure, and we do not adopt it the remaining analysis.

Regardless of whether or not an observed process is truly periodic, there is an obvious limitation to any method that attempts to fit a periodic function to data that span only a small fraction of the hypothesized period. Any noise superposed on an otherwise smooth radial velocity curve, such as that which is evident in Arp 102B and apparently in 3C 390.3 as well, could grossly change the derived value or lower limit to the period. This is a weakness of both Gaskell’s study of 3C 390.3 and ours. The lower limits on the period and the mass that we derive are not necessarily secure ones if there are, superimposed on the binary motion, occasional velocity variations of unknown origin with a typical amplitude of 10^3 km s^{-1} . The possibility of such contamination constitutes a caveat to our otherwise clean rejection of the binary broad-line region model for the three objects. However, because we are unable to suggest a secondary mechanism for such large radial velocity variations, we find it more reasonable to conclude that the observed changes are due to a single as yet unexplained cause, for which binary orbital motion is an unlikely explanation.

The lower limits to the orbital periods and the corresponding projected velocity amplitudes were used to determine the lower limit on the mass in each case. These limits are summarized in Table 1. The corresponding mass ratios and lower limits on the binary separation are also given. In the following paragraphs we discuss the results for each object individually, paying attention to its idiosyncrasies.

4.1. Arp 102B

The minimum total mass obtained from fitting the velocity curve of Arp 102B is $5.1 \times 10^9 M_{\odot}$, under the assumption that $q = 1$. This is higher than that reported by Halpern & Filippenko (1988, 1992), which is an expected benefit of the lengthening time span of the observations. The constraints that we derive for Arp 102B are not as restrictive as they might have been, because we still do not make use of the red peak of its $H\alpha$ line. The velocity of the red peak cannot be measured reliably because it coincides with the [S II] $\lambda\lambda 6717, 6731$ doublet. This complication also

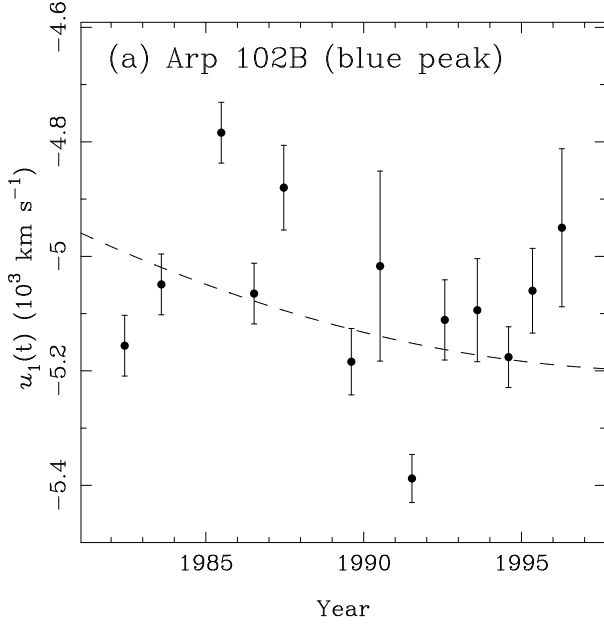
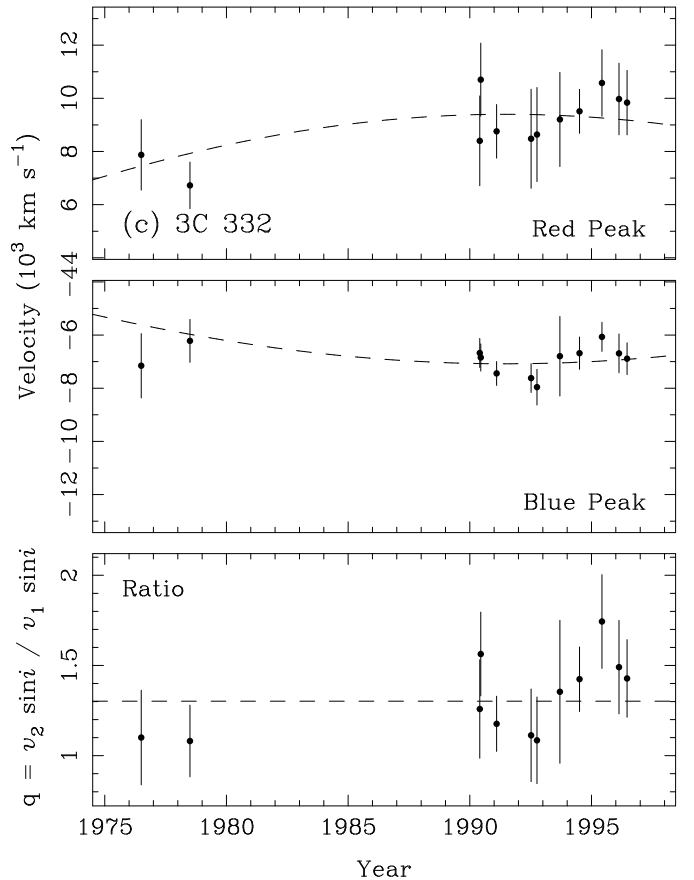
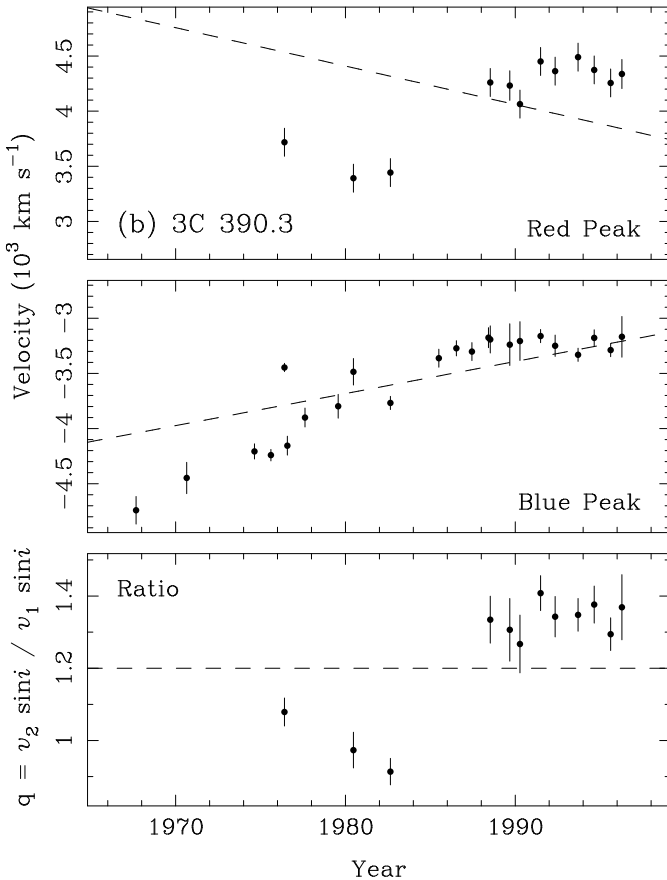


FIGURE 4— Annually-averaged radial velocity curves with the best-fitting binary models (dashed lines) overlaid. The data points represent the average of all measurements made from both the H α and the H β profiles from the same year. (a) In the case of Arp 102B, only the fit to the radial velocity curve of the blue peak is shown since these are the only reliable data. In the case of the other two objects, the simultaneous fits to the radial velocity curves of both peaks are shown. The lower panels in (b) and (c) show the variation of the red/blue velocity ratios with time; the horizontal dashed line shows the velocity ratio derived from the best-fitting model. The error bars in (a) and (b) are computed statistically as described in the text; they represent the dispersion within a year rather than the error in the annual mean. The error bars in (c) represent the uncertainties in individual measurements.



prevents us from assigning a precise value to the mass ratio. Nevertheless, we can conclude from the asymmetry of the line profile and from the apparent coincidence of the red peak of H α with the [S II] doublet that the hypothesized mass ratio must be about 1.5, similar to the two other objects whose red peaks are easily measured. If so, the minimum mass would be $1.3 \times 10^{10} M_{\odot}$, about twice as large as that derived under the conservative assumption of equal black hole masses. In Table 1 we report the limits that correspond to $q = 1.5$, which we consider a more reasonable and realistic assumption than $q = 1$.

The radial velocity curve of Arp 102B presented in Figure 2a shows considerable scatter, of order 300 km s^{-1} about a mean of 5100 km s^{-1} . As we have argued, this is likely the result of intrinsic profile variations on short time scales which probably dominate the uncertainty in the location of the peak. If we use this argument as a basis for rejecting some data points from the analysis, a minimum mass can be derived that is higher than those we report in Table 1. This is a second reason why the lower mass limits listed for Arp 102B in Table 1, which are derived using *all* of the points in each velocity curve, are the most conservative (lowest) that one could infer. In summary, we consider $10^{10} M_{\odot}$ a realistic lower limit on the total mass of the black holes in Arp 102B in the binary broad-line region scenario.

4.2. 3C 390.3

The radial velocity curve of the *blue* H β peak of 3C 390.3 presented by Gaskell (1996a) shows that the peak drifted systematically by about 1700 km s^{-1} between 1968 and 1988. This behavior was interpreted by Gaskell as the signature of orbital motion, with a most likely period of 300 years and a total binary mass of $6.6 \times 10^9 M_{\odot}$. Our newer data, however, show that this trend did not continue after 1988. To illustrate the subsequent deviation, we plot in Figure 5 the data and best binary orbit model of Gaskell (1996a) and superpose our additional data for comparison. It is clear from this figure that the velocities after 1988 do not follow the extrapolation of the binary model that fits the velocities between 1968 and 1988. The direction of the deviation disfavors *any* orbital model for the radial velocity variations observed over the full time span. Furthermore, the observed trend in the velocity of the *red* peak of H α is inconsistent with orbital models: in the binary orbital motion picture, the two peaks should drift in opposite directions, which is flatly contradicted by the observations (Figure 4b).

The year 1989 coincided with a revealing development in the line profile of 3C 390.3 which constitutes another obstacle to the binary broad-line region interpretation. Previously the displaced peaks had round tops, and were easily located by fitting symmetric functions. But in 1989 the blue peak developed the sharp cusp shown in Figure 3. We are confident in the reality of this feature because it lies 37 \AA blueward of the head of the telluric B-band, and because it persisted through 1990. By 1991, the blue peak had resumed its more normal, rounded appearance. In addition to complicating the measurement of “a radial velocity,” this cusplike feature is evidence of a well ordered velocity field, and not the random distribution of cloud orbits that is implicit in the binary scenario. It is perhaps significant that the appearance of this transient feature coincided with the ending of the radial velocity trend noticed by Gaskell (1996a). Apparently, there exists a dynamical process, one not consistent with binary orbital motion, that is responsible for shaping the line profile.

Despite these warnings that a binary broad-line region model is unsuited to 3C 390.3, if we persist and fit its velocity curve to a binary orbit, we obtain the period and mass limits given in Table 1. The mass limit of $4.2 \times 10^{10} M_{\odot}$ can be made more restrictive by using information on the inclination of the orbital plane. From the observations of superluminal motion in 3C 390.3 by Alef et al. (1994, 1996), Eracleous, Halpern, & Livio (1996) derive an upper limit to the inclination angle of the jet to the line of sight of $i < 33^{\circ}$. Assuming that the plane of the orbit is perpendicular to the axis of the radio jet, this limit implies that $M > 2.6 \times 10^{11} M_{\odot}$, a value 40 times larger

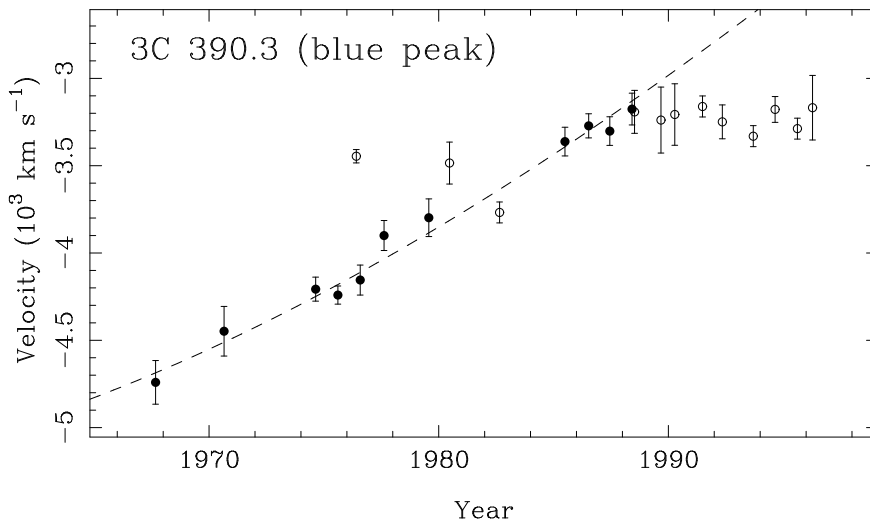


FIGURE 5 – An expanded view of the radial velocity curve of the blue peak of 3C 390.3. The filled circles are the data of Gaskell (1996a) with error-in-the-mean error bars, while the open circles are our own data with r.m.s.-dispersion error bars. The dashed line shows Gaskell’s fit to the data prior to 1988; it corresponds to a period of 300 yr. The radial velocities measured after 1988 clearly do not follow the extrapolation of the fit based on data prior to 1988.

than that derived by Gaskell⁵ and large enough to render the assumed model for the emission line implausible (see §5).

4.3. 3C 332

Because 3C 332 was not observed as frequently as the other two targets, it is not possible to compute statistical error bars (using the annual dispersion of individual measurements) for all of its radial velocity data points. We therefore adopt the individual measurement uncertainties. Figure 4c shows these measurements and associated error bars, along with the best-fitting binary orbit model. This is the only object for which a binary orbit model produces a formally acceptable fit, mainly because of the large error bar associated with each measurement. Even though the velocity curve of 3C 332 is not as well sampled as those of the other two objects, it still yields an interesting mass constraint, $M > 1.5 \times 10^{10} M_{\odot}$, on the total mass of a supermassive binary that this object may harbor. Two observational factors combine to achieve this sensitive limit. First, the time spanned by the radial velocity curve is quite long, and second, the separation between the twin peaks of H α is almost twice that of the other two objects. We note that the large velocity

⁵ The derivation of the mass of the binary by Gaskell (1996a) also took into account the inclination of the orbit using a jet inclination of $i = 29^{\circ}$. That estimate was made by Ghisellini et al. (1993) from a combination of superluminal motion data and a synchrotron self-Compton model for the X-ray emission. The method is similar but not identical to that of Eracleous et al. (1996), and the data were taken from an independent source. The resulting estimates are consistent with each other.

separation between the two peaks is *not* necessarily an indication of an extremely massive binary or a small binary separation. The *observed* velocity separation between the two peaks is

$$\Delta v_{\text{peaks}} = \left(\frac{GM}{a} \right)^{1/2} \sin i \sin \varphi, \quad (7)$$

where a is the binary separation and φ is the orbital phase ($\varphi = 0$ corresponds to inferior conjunction of the primary). It is clear from equation (7) that the velocity widths of the lines depend at least as sensitively on the observer’s perspective (i.e., the orbital inclination and phase) as they do on the intrinsic properties of the binary (mass and separation).

5. DISCUSSION

A binary broad-line region interpretation of double-peaked emission lines implies, through the simple dynamical arguments of the preceding sections, binary black hole masses greater than $10^{10} M_{\odot}$ in all three of the objects studied. The mass limits that we derive are the lowest reasonable limits, since throughout our analysis we have tried to err on the side of caution. These very large required masses render a binary interpretation very unlikely for a number of reasons. In this section, we discuss how these assumed masses conflict with other observations and with theory.

First, a mass of the order of $10^{10} M_{\odot}$ is well in excess of the masses of central black holes in active and non-active galaxies that have been measured by means of circular gas velocities or stellar kinematics. Examples of such mass determinations in *active* galaxies include $3.5 \times 10^7 M_{\odot}$ in NGC 4258 (Miyoshi et al. 1995), $5 \times 10^8 M_{\odot}$ in NGC 4261 (Ferrarese, Ford, & Jaffe 1996), $10^9 M_{\odot}$ in NGC 4594 (Kormendy et al. 1996a), and $2 \times 10^9 M_{\odot}$ in M87 (Harms et al. 1994). Examples of non-active galaxies with a well-determined nuclear black hole mass are NGC 3115 ($M \approx 2 \times 10^9 M_{\odot}$; Kormendy et al. 1996b), NGC 4486B ($M \approx 6 \times 10^8 M_{\odot}$; Kormendy et al. 1997), and M32 ($M \approx 3 \times 10^6 M_{\odot}$; van der Marel et al. 1997). Certainly these observational techniques suffer no technical difficulties that would prevent them from detecting single black holes of $10^{10} M_{\odot}$. In fact, one would expect very massive black holes to be easily detectable by the above techniques. Why should the most massive black holes be found only in binaries?

A second objection to such extremely massive binaries is the remarkable coincidence that would be required for *two* record-setting black holes, of nearly equal mass, to find themselves in the same galaxy and emitting nearly the same Balmer-line luminosity. One such system could be dismissed as unique and unrepresentative, but there are several such systems in our neighborhood. It is more reasonable to interpret the approximate symmetry in velocity and flux of these double-peaked emission lines as the workings of a *single*, less massive object, even though we may not yet understand the process that is responsible.

A third, and potentially serious weakness of the binary model is that the very large requisite masses strain against *upper* limits that can be derived from variability time scales, most notably via X-ray observations. If we accept that one or both of the members of the hypothesized binary is responsible for the AGN’s X-ray emission and its variability, then the size r of either emission region can be no greater than $c\Delta t$, where Δt is the observed variability time scale. Because the X-ray emitting region is thought to occupy the inner parts of an accretion disk, up to $r \approx 10 r_g$ (where $r_g \equiv GM/c^2$), the implied upper limit to the mass of the black hole is

$$M < 1.7 \times 10^9 \left(\frac{\Delta t}{1 \text{ day}} \right) \left(\frac{r}{10 r_g} \right)^{-1} M_{\odot}. \quad (8)$$

One of the best studied AGN X-ray light curves is that of 3C 390.3. During long-term monitoring by *ROSAT*, 3C 390.3 displayed large-amplitude flares with a minimum doubling time scale of 9

days (Leighly et al. 1997*a, b*). This behavior implies a maximum black hole mass of $1.5 \times 10^{10} M_{\odot}$, uncomfortably low compared to the lower limit in Table 1. One can relieve this strain by invoking relativistic motion for the source of the X-rays, which would make the *intrinsic* variability time scale longer than the observed one. However, the similarity between the X-ray spectra of 3C 390.3 and those of ordinary Seyfert galaxies, most notably the presence of an Fe K α line at the rest energy in the frame of the galaxy (Eracleous et al. 1996), argues that the X-ray source in 3C 390.3 is not beamed. We consider the observed rapid X-ray variability to be a strong argument against the association of the X-ray source with a black hole more massive than $10^{10} M_{\odot}$ in 3C 390.3, and certainly against masses greater than $10^{11} M_{\odot}$ that would be required if the orbital inclination were less than 33° . The X-ray variability properties of our other two objects have not yet been studied, but similar monitoring observations of Arp 102B and 3C 332 could be very effective in disallowing the large masses required for them by the binary broad-line region model.

A fourth issue that needs to be revisited if the mass of the hypothesized binary is of order $10^{10} M_{\odot}$ or larger is the decay of the orbit by gravitational radiation, which is the final process in the coalescence of the binary. The expression for the time to coalescence given by Lightman et al. (1979) can be written as

$$T_{\text{gr}} = 5.7 \times 10^8 \frac{(1+q)^2}{q} \frac{a_{\text{pc}}^4}{M_{10}^3} \text{ yr}, \quad (9)$$

where M_{10} is the mass of the binary in units of $10^{10} M_{\odot}$ and a_{pc} is the binary separation in pc. Upper limits on the binary coalescence times can be obtained using the minimum masses derived here and upper limits on the binary separation from VLBI observations of the radio cores of these objects. In particular, observations of 3C 390.3 and Arp 102B by Alef et al. (1994, 1996) and Biermann et al. (1981) show that the radio cores are unresolved and yield upper limits to the core sizes of 1.4 pc and 0.4 pc respectively. The corresponding VLBI maps have very high dynamic range so that close radio doubles with a large intensity contrast would have been detected had they been separated by more than the core sizes given above. The implied upper limits to the coalescence times are 7×10^7 yr for Arp 102B and 3×10^8 yr for 3C 390.3. If instead the orbital separation of Arp 102B is as small as that given in Table 1, which is highly desirable to minimize the mass, the coalescence times could be as small as 9×10^6 yr. The corresponding coalescence time of 3C 332 is only 2×10^6 yr. Since the coalescence time is such a sensitive function of the mass of the system, it is surprising that all three objects in our collection have large masses. Objects with masses that are even a factor of 2 smaller would have almost an order of magnitude longer coalescence times and hence they would be more likely to be found. We note that the observed velocity separation of the two peaks does not necessarily imply a shorter lifetime [cf., equation (7)]. Moreover, in the case of 3C 390.3 the inferred minimum separation of the hypothesized binary is comparable to the spatial resolution of the available VLBI map, which implies that the binary should have been resolved. If the mass of the binary in 3C 390.3 is indeed $2.6 \times 10^{11} M_{\odot}$, according to the upper limit on the inclination, the binary separation is 2.3 pc, easily resolvable in the VLBI map of Alef et al. (1994, 1996).

There are additional problems with the binary broad-line region interpretation that are unrelated to the large masses required. One that has been recognized for some time was first noted by M. V. Penston, and summarized in footnote 3 of Chen, Halpern, & Filippenko (1989). The line profile of a binary broad-line region should not consist of two widely displaced peaks, because the velocity dispersion of gas bound to each black hole should be *greater* than its binary orbital velocity. Thus, the double line profile should be more highly blended. In defense of the model, the possibility of fine tuning between the opposing forces of gravity and radiation pressure has been invoked to decrease the line width of each individual broad-line region (Gaskell 1996*a*, drawing from the model of Mathews 1993). We are unable to judge how reasonable it is to assume such a balance.

Finally, recent results from *HST* ultraviolet spectroscopy of Arp 102B provide a new and striking view of this object that offers no support for a binary broad-line region interpretation (Halpern et al. 1996). In all the ultraviolet (and visible) emission lines, there is present an “ordinary” broad-line component at zero velocity. In contrast, the double-peaked component is strong only in the Balmer lines and in Mg II, but is completely absent in Ly α and other high-ionization lines, indicating an unusually low level of ionization in the double-peaked components. Evidently, extreme physical conditions are present in the high velocity gas. A model in which two black holes are surrounded by individual broad-line regions does not account for the unusual line intensity ratios in either of the displaced peaks of Arp 102B.

6. EPILOGUE

Although we have found no evidence to support the binary broad-line region interpretation of double-peaked emitters from long-term monitoring of three objects, this does not mean that a binary model cannot account for the emission line profiles of some of the many other AGNs with either single or double displaced peaks. Our three targets were chosen precisely because the very large velocity widths of their lines enable meaningful results to be obtained in just a couple of decades. Emission-line peaks with velocities significantly less than these, such as in OX 169 (Stockton & Farnham 1991), may still arise in a less massive spectroscopic binary, even if the peaks appear stationary for many years. OX 169 and similar objects remain plausible binary candidates. We do conclude, however, that the *transient* double-peaked emission lines that were recently discovered in an additional trio of objects, namely NGC 1097 (Storchi-Bergmann, Baldwin, & Wilson 1993; Storchi-Bergmann et al. 1995, 1997), Pictor A (Halpern & Eracleous 1994; Sulentic et al. 1995), and M81 (Bower et al. 1996), are *not* likely to originate in binary broad-line regions. These suffer most of the same objections that apply to the persistent double-peaked emitters. Their peaks are too symmetric and widely spaced, and at least two of these objects, M81 and Pictor A, have long possessed ordinary broad lines at zero velocity, as well as luminous and variable X-ray emission that does not appear to have increased in concert with their new emission-line components. In addition, the very transient nature of these displaced peaks, appearing and disappearing together as they do, argues against an origin in independent accreting systems. Because these transient double-peaked emitters are so nearby, it seems likely that they are quite common among AGNs, outnumbering the persistent ones by a large factor. Our understanding of both groups would greatly benefit if they could be “unified” by the same mechanism.

We emphasize that even in the three objects for which we have derived strong constraints against the binary broad-line region model, we have not ruled out the *existence* of a supermassive binary black hole, but only the scenario in which separate black holes are responsible for the two displaced emission-line peaks. It is still possible that binaries *less* massive than the limits listed in Table 1 lurk in these AGNs, if the emission-line source is associated with only one of the black holes. The observational signature of such a system would be an equal modulation of the velocities of the two peaks in the *same* direction. We have not yet seen any such evidence of a *single-lined* spectroscopic binary, although the relative motions of the two emission-line peaks of 3C 390.3 shown in Figure 4b might be compatible with such a description. Taking into account possible random velocity variations of $K \simeq 1000 \text{ km s}^{-1}$ resulting from unexplained changes in the line profiles, we estimate that we would be sensitive to systems with mass ratios $q < 12 (K/1000 \text{ km s}^{-1})^{-1} (M_9/a_{17})^{1/2}$ for orbital periods comparable to the time span of our data. Another possibility which remains open is that some AGNs harbor supermassive binaries with a single, circumbinary broad-line region. We speculate that an observational signature of these systems would be periodic episodes of brightening caused by a modulated accretion rate (c.f., Artimowicz & Lubow 1996).

Even though we judge that the arguments against the binary broad-line region model for the objects that we have studied are already quite strong, there are powerful additional tests that could

be performed. First, there exists a large amount of spectroscopic data on 3C 390.3 obtained in conjunction with a one-year reverberation monitoring campaign (Dietrich et al. 1997). If the $H\alpha$ emission line shows reverberation in response to continuum variations, and if *both* sides of the line respond with little or no delay between them, then a binary broad-line region model is virtually ruled out, since the required orbital separation is 0.3 pc in Gaskell’s (1996*a*) analysis, or greater than 1.5 pc in ours. We eagerly await the results of these observations. Second, it is possible in principle to detect absolute motions of compact cores with a precision of tens of microarcseconds using relative astrometry between widely spaced VLBI sources (Lara et al. 1996). If the compact core of an object like 3C 390.3 were really moving at a velocity of $5,000 \text{ km s}^{-1}$ relative to its host galaxy, then a displacement of 0.1 milliarcseconds would be expected in 30 years. In a time comparable to the length of our optical spectroscopic studies, independent evidence for or against binary orbital motion could thus be obtained from VLBI astrometry.

We have refrained in this paper from speculating upon the actual origin of these double-peaked emission lines. That is a much more difficult task than the falsification of one particular, albeit important, model. A discussion of more plausible models is presented in those same papers that contain the detailed descriptions of our spectra and their variability (Newman et al. 1997; Gilbert et al. 1997).

ACKNOWLEDGMENTS

We are indebted to all the Lick Observatory observers who allowed us to use old data that they have been saving for the past two decades. In particular, we are grateful to D. E. Osterbrock, M. M. Phillips, and S. A. Grandi. We also thank W. Zheng for passing on many of the old Lick spectra to us in a convenient, electronic form, and the referee, C. M. Gaskell, for his thoughtful comments. M.E. acknowledges support by Hubble Fellowship grant HF-01068.01-94A. A.M.G. and J.A.N. acknowledge support from a Eugene Cota-Robles and a National Science Foundation Fellowship respectively. This work was also partly supported by NASA grant G0-06097-94A from the Space Telescope Science Institute (operated by AURA, Inc., under NASA contract NAS5-26555).

REFERENCES

- Alef, W., Preuss, E., Kellerman, K. I., Wu, S. Y., & Qiu, Y. H. 1994, in *Compact Extragalactic Radio Sources*, NRAO Workshop No. 23, ed. J. A. Zensus & K. I. Kellerman (Green Bank: NRAO), 55
- Alef, W., Wu, S. Y., Preuss, E., Kellerman, K. I., & Qiu, Y. H. 1996, *A&A*, 308, 376
- Artimowicz, P. & Lubow, S. H. 1996, *ApJ*, 467, L77
- Begelman, M. C., Blandford, R. D., & Rees, M. J. 1980, *Nature*, 287, 307
- Biermann, P., Preuss, E., Kronberg, P. P., Schilizzi, R. T., & Shaffer, D. B. 1981, *ApJ*, 250, L49
- Bower, G. A., Wilson, A. S., Heckman, T. M., & Richstone, D. O. 1996, *AJ*, 111, 1901
- Chen, K., Halpern, J. P., & Filippenko, A. V. 1989, *ApJ*, 339, 742
- Dietrich, M. et al. 1997, *ApJ*, submitted
- Eracleous, M. 1997, *Adv Space Res*, in press
- Eracleous, M., & Halpern, J. P. 1994, *ApJS*, 90, 1
- Eracleous, M., Halpern, J. P., & Livio, M. 1996, *ApJ*, 459, 89
- Ferrarese, L., Ford, H. C., & Jaffe, W. 1996, *ApJ*, 470, 444
- Gaskell, C. M. 1983, in *Proc. 24th Liège Int. Astrophys. Colloq., Quasars and Gravitational Lenses (Cointe-Ougree: Univ. Liège)*, 473
- . 1988, in *Active Galactic Nuclei*, ed. H. R. Miller & P. J. Witta (Berlin: Springer), 61
- . 1996*a*, *ApJ*, 464, L107
- . 1996*b*, in *Jets from Stars and Galactic Nuclei*, ed. W. Kundt, (Berlin: Springer), 165

- Gaskell, C. M. & Snedden, S. A. 1997, in *Emission Lines in Active Galaxies: New Methods and Techniques*, ed. B. M. Peterson, F.-Z. Cheng, & A. S. Wilson (San Francisco: ASP), 193
- Ghisellini, G., Padovano, P., Celotti, A., & Maraschi, L. 1993, *ApJ*, 407, 65
- Gilbert, A. M., Eracleous, M., Halpern, J. P., & Filippenko, A. V. 1997, in preparation
- Grandi, S. A., & Osterbrock, D. E. 1978, *ApJ*, 220, 783
- Grandi, S. A., & Phillips, M. M. 1979, *ApJ*, 232, 659
- Halpern, J. P., & Eracleous, M. 1994, *ApJ*, 433, L17
- Halpern, J. P., Eracleous, M., Filippenko, A. V., & Chen, K. 1996, *ApJ*, 464, 704
- Halpern, J. P., & Filippenko, A. V. 1988, *Nature*, 331, 46
- . 1992, in *Testing the AGN Paradigm*, ed. S. S. Holt, S. G. Neff, & C. M. Urry, *AIP Conf. Proc.* 254, (New York: AIP), 57
- Harms, R., et al., 1994, *ApJ*, 435, L35
- Hoffmeister, C., Richter, G., & Wenzel, W. 1985, *Variable Stars* (Berlin: Springer)
- Kormendy, J., et al. 1996*a*, *ApJ*, 459, L57
- . 1996*b*, *ApJ*, 473, L91
- . 1997, *ApJ*, 482, L139
- Lampton, M., Margon, B., & Bowyer, S. 1976, *ApJ*, 208, 177
- Lara, L., Marcaide, J. M., Alberdi, A., & Guirado, J. C. 1996, *A&A*,
- Lauer, T. R., et al. 1991, *ApJ*, 369, L41
- . 1992, *AJ*, 103, 703
- . 1995, *AJ*, 110, 2622
- Leighly, K. M., & O’Brien, P. T. 1997*a*, *ApJ*, 481, L15
- Leighly, K. M., O’Brien, P. T., Edelson, R., George, I. M., Malkan, M. A., Matsuoka, M., Mushotzky, R. F., & Peterson, B. M. 1997*b*, *ApJ*, 483, 767
- Lightman, A. P., Press, W. H., Price, R. H., & Teukolsky, S. A. 1979, *Problem Book in Relativity and Gravitation*, (Princeton: Princeton U. Press), 495
- Mathews, W. G. 1993, *ApJ*, 412, L17
- Miyoshi, M., Moran, J. M., Herrnstein, J. R., Greenhill, L. J., Nakai, N., Diamond, O. J., & Inoue, M. 1995, *Nature*, 373, 127
- Newman, J. A., Eracleous, M., Halpern, J. P., & Filippenko, A. V., 1997, *ApJ*, in press
- Oke, J. B. 1987, in *Superluminal Radio Sources*, ed. J. A. Zensus & T. J. Pearson (Cambridge: Cambridge University Press), 267
- Polnarev, A. G., & Rees, M. J. 1994, *A&A*, 283, 301
- Quinlan, G. D. 1996, *New Astronomy*, 1, 35
- Stauffer, J., Schild, R., & Keel, W. 1983, *ApJ*, 270, 465
- Stockton, A., & Farnham, T. 1991, *ApJ*, 371, 525
- Storchi-Bergmann, T., Baldwin, J. A., & Wilson, A. S. 1993, *ApJ*, 410, L11
- Storchi-Bergmann, T., Eracleous, M., Livio, M., Wilson, A. S., Filippenko, A. V., & Halpern, J. P. 1995, *ApJ*, 443, 617
- Storchi-Bergmann, T., Ruiz, T. R., & Eracleous, M. 1997, *Adv Space Res*, in press
- Sulentic, J. W., Marziani, P., Zwitter, T., & Calvani, M. 1995, *ApJ*, 438, L1
- van der Marel, R. P., de Zeeuw, P. T., Rix, H.-W., & Quinlan, G. D. 1997, *Nature*, 385, 610
- Wade, R. A. & Horne, K. 1988, *ApJ*, 324, 411
- Zheng, W., Pérez, E., Grandi, S. A., & Penston, M. V. 1995, *AJ*, 109, 2355